

Dynamic buckling response of temperature-dependent functionally graded-carbon nanotubes-reinforced sandwich microplates considering structural damping

Maryam Shokravi^{*1} and Nader Jalili²

¹Buein Zahra Technical University, Buein Zahra, Qazvin, Iran

²Piezoelectric Systems Laboratory, Department of Mechanical and Industrial Engineering, Northeastern University, Boston, Massachusetts 02115, USA

(Received September 7, 2017, Revised August 18, 2017, Accepted October 26, 2017)

Abstract. This research deals with the nonlocal temperature-dependent dynamic buckling analysis of embedded sandwich micro plates reinforced by functionally graded carbon nanotubes (FG-CNTs). The material properties of structure are assumed viscoelastic based on Kelvin–Voigt model. The effective material properties of structure are considered based on mixture rule. The elastic medium is simulated by orthotropic visco-Pasternak medium. The motion equations are derived applying Sinusoidal shear deformation theory (SSDT) in which the size effects are considered using Eringen's nonlocal theory. The differential quadrature (DQ) method in conjunction with the Bolotin's methods is applied for calculating resonance frequency and dynamic instability region (DIR) of structure. The effects of different parameters such as volume percent of CNTs, distribution type of CNTs, temperature, nonlocal parameter and structural damping on the dynamic instability of visco-system are shown. The results are compared with other published works in the literature. Results indicate that the CNTs have an important role in dynamic stability of structure and FGX distribution type is the better choice.

Keywords: dynamic buckling; FG-CNT; nanocomposite sandwich micro plate; SSDT; viscoelastic

1. Introduction

Nanocomposite materials are composed of different functional components such as polymer, nanoparticle and ligands, with at least one component having nanometer dimensions. Typically, the dispersion of nanoparticles in polymer matrices is problematic and the nanoparticles tend to phase separate or aggregate in the polymer matrix. Nanoparticle agglomeration and phase separation from the host polymer usually results in poor process ability of films and a high defect density. Moreover, physical properties of the composite material are very sensitive to particle dispersion within the nanocomposite (Mori and Tanaka, 1973).

Mechanical analysis of nano/micro plates were taken up by several researchers lately. A finite element model based on an improved higher order zigzag plate theory was developed by Pandit *et al.* (2009) for bending and vibration response of soft core sandwich plates. Buckling and free vibration of magneto-electro-elastic nanoplate resting on Pasternak foundation was presented by Li *et al.* (2014) based on nonlocal Mindlin theory. Applying different nonlocal shear deformable plate theories, Kiani (2014) carried out the free vibration of conducting nanoplates

exposed to unidirectional in-plane magnetic fields. Ke *et al.* (2015) presented free vibration of nonlocal piezoelectric nanoplates using differential quadrature method (DQM). A simple four-variable trigonometric shear deformation theory considering the effects of transverse shear deformation and rotary inertia was evaluated by Atteshamuddin and Yuwaraj (2017) for the free vibration analysis of antisymmetric laminated composite and soft core sandwich plates. The magneto-rheological visco-elastomer (MRVE) was used by Ying *et al.* (2017) as a smart core to control the stochastic micro-vibration of a sandwich plate with supported mass.

With respect to the developed works for nanocomposite structures, there are many works in recent years. Nonlinear bending of FG-CNTRC plates was presented by Shen (2009), who considered the size-dependent and temperature dependent material properties of single-wall CNTs. The bending and free flexural vibration behavior of sandwich plates with CNT reinforced face sheets were investigated by Natarajan *et al.* (2014). Abdollahzadeh Shahrababaki and Alibeigloo (2014) studied the three-dimensional free vibration of CNT reinforced composite rectangular orthotropic plates with various boundary conditions. Four-unknown quasi-3D shear deformation theory for advanced composite plates was investigated by Mantari and Guedes Soares (2014). Rafiee *et al.* (2014) worked on non-linear dynamic stability of piezoelectric FG-CNTRC plates with initial geometric imperfection. Wattanasakulpong and Chaikittrirana (2015) carried out the exact solutions for static and dynamic analyses of CNTRC plates with

*Corresponding author, Ph.D.
E-mail: Maryamshokravi10@yahoo.com;
Maryamshokravi10@bzte.ac.ir

Pasternak elastic foundation. Phung-Van *et al.* (2017) presented the iso-geometric analysis of FG-CNTRC plates using higher-order shear deformation theory. Chetan *et al.* (2017) studied modelling of the interfacial damping due to nanotube agglomerations in nanocomposites.

However, to date, no report has been found in the literature on dynamic stability of viscoelastic nanocomposite micro plates. Motivated by these considerations, in order to improve optimum design of nanostructures, we aim to present a realistic model for temperature-dependent dynamic instability of micro plates reinforced with FG-CNTs. The structural damping effects are assumed by Kelvin–Voigt model. The surrounding elastic medium is simulated by orthotropic visco-Pasternak foundation. The mixture rule is applied for obtaining the equivalent material properties of structure. The motion equations are obtained using SSDT and energy method considering size effects. DQ method is used to calculate the resonance frequency and DIR of structure. The effects of different parameters such as volume percent of CNTs, distribution type of CNTs, temperature, nonlocal parameter and structural damping on the dynamic instability of visco-system are elucidated.

2. Mixture rule

As shown in Fig. 1, a CNTRC visco-plate with length a , width b and thickness h is considered. The CNTRC plate is surrounded by an orthotropic elastomeric temperature-dependent medium which is simulated by K_W , $K_{g\xi}$ and $K_{g\eta}$ correspond Winkler foundation parameter, shear foundation parameters in ξ and η directions, respectively. Four types of CNTRC plates namely as uniform distribution (UD) along with three types of FG distributions (FGA, FGO, FGX) of CNTs along the thickness direction of a CNTRC plate is considered.

In order to obtain the equivalent material properties two-phase Nanocomposites (i.e., polymer as matrix and CNT as reinforcer), the rule of mixture is applied. According to mixture rule, the effective Young and shear moduli of CNTRC plate can be written as (Shen 2009)

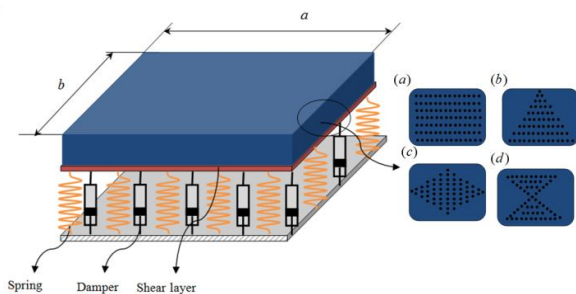


Fig. 1 Configurations of the SWCNT distribution in a CNTRC plates. (a) UD CNTRC plate, (b) FG-A CNTRC plate, (c) FG-O CNTRC plate and (d) FG-X CNTRC plate

$$E_{11} = \eta_1 V_{CNT} E_{r11} + (1 - V_{CNT}) E_m, \tag{1}$$

$$\frac{\eta_2}{E_{22}} = \frac{V_{CNT}}{E_{r22}} + \frac{(1 - V_{CNT})}{E_m}, \tag{2}$$

$$\frac{\eta_3}{G_{12}} = \frac{V_{CNT}}{G_{r12}} + \frac{(1 - V_{CNT})}{G_m}, \tag{3}$$

where E_{r11} , E_{r22} and G_{r11} indicate the Young's moduli and shear modulus of SWCNTs, respectively, and E_m , G_m represent the corresponding properties of the isotropic matrix. The scale-dependent material properties, η_j ($j = 1, 2, 3$), can be calculated by matching the effective properties of CNTRC obtained from the MD simulations with those from the rule of mixture. V_{CNT} and V_m are the volume fractions of the CNTs and matrix, respectively, which the sum of them equals to unity. The uniform and three types of FG distributions of the CNTs along the thickness direction of the CNTRC plates take the following forms

$$UD: V_{CNT} = V_{CNT}^*, \tag{4}$$

$$FGV: V_{CNT}(z) = \left(1 - \frac{2z}{h}\right) V_{CNT}^*, \tag{5}$$

$$FGO: V_{CNT}(z) = 2 \left(1 - \frac{2|z|}{h}\right) V_{CNT}^*, \tag{6}$$

$$FGX: V_{CNT}(z) = 2 \left(\frac{2|z|}{h}\right) V_{CNT}^*, \tag{7}$$

where

$$V_{CNT}^* = \frac{w_{CNT}}{w_{CNT} + (\rho_{CNT} / \rho_m) - (\rho_{CNT} / \rho_m) w_{CNT}}, \tag{8}$$

where w_{CNT} , ρ_m and ρ_{CNT} are the mass fraction of the CNT, the densities of the matrix and CNT, respectively. Similarly, the thermal expansion coefficients in the longitudinal and transverse directions respectively (α_{11} and α_{22}) and the density (ρ) of the CNTRC plates can be determined as

$$\rho = V_{CNT}^* \rho_r + V_m \rho_m, \tag{9}$$

$$\alpha_{11} = V_{CNT}^* \alpha_{r11} + V_m \alpha_m, \tag{10}$$

$$\alpha_{22} = (1 + \nu_{r12}) V_{CNT} \alpha_{r22} + (1 + \nu_m) V_m \alpha_m - \nu_{12} \alpha_{11}, \tag{11}$$

where ν_{r12} and ν_m are Poisson’s ratios of the CNT and matrix, respectively. In addition, α_{r11} , α_{r22} and α_m are the thermal expansion coefficients of the CNT and matrix, respectively. It should be noted that ν_{12} is assumed as constant over the thickness of the FG-CNTRC plates.

3. Visco-nonlocal-sinusoidal theories

In the Eringen’s nonlocal elasticity model, the stress state at a reference point in the body is regarded to be dependent not only on the strain state at this point but also on the strain states at all of the points throughout the body. The constitutive equation of the nonlocal elasticity is (Eringen 1983)

$$(1 - (e_0 a)^2 \nabla^2) \sigma_{ij} = C_{ijkl} \epsilon_{kl}, \tag{12}$$

where the parameter $e_0 a$ denotes the small scale parameter, and ∇^2 is the Laplace operator. The constitutive equation for stresses σ and strains ϵ matrix in thermal environment may be written as follows

$$(1 - (e_0 a)^2 \nabla^2) \begin{Bmatrix} \sigma_{xx} \\ \sigma_{yy} \\ \sigma_{xz} \\ \sigma_{yz} \end{Bmatrix} = \begin{bmatrix} C_{11}(z,T) & C_{12}(z,T) & 0 & 0 & 0 \\ C_{21}(z,T) & C_{22}(z,T) & 0 & 0 & 0 \\ 0 & 0 & C_{44}(z,T) & 0 & 0 \\ 0 & 0 & 0 & C_{55}(z,T) & 0 \\ 0 & 0 & 0 & 0 & C_{66}(z,T) \end{bmatrix} \begin{Bmatrix} \epsilon_{xx} - \alpha_{11} \Delta T \\ \epsilon_{yy} - \alpha_{22} \Delta T \\ \gamma_{yz} \\ \gamma_{xz} \\ \gamma_{xy} \end{Bmatrix}, \tag{13}$$

where C_{ij} denotes temperature-dependent elastic coefficients. Noted that C_{ij} and α_{11}, α_{22} may be obtained using rule of mixture (i.e., Eqs. (1)-(7)). All materials exhibit some viscoelastic response. According to Kelvin–Voigt (Lei *et al.* 2013) at real life, nano structure mechanical properties depend on the time variation. This model represents, as the stress is released, the material gradually relaxes to its undeformed state. By considering this model, we have

$$C_{ij} = C_{ij} \left(1 + g \frac{\partial}{\partial t} \right), \tag{14}$$

where g is structural damping constant. Based on the SSdT, the displacement field can be written as (Thai and Vo 2013)

$$U_1(x, y, z, t) = U(x, y, t) - z \frac{\partial W_b}{\partial x} - f \frac{\partial W_s}{\partial x}, \tag{15}$$

$$U_2(x, y, z, t) = V(x, y, t) - z \frac{\partial W_b}{\partial y} - f \frac{\partial W_s}{\partial y}, \tag{16}$$

$$U_3(x, y, z, t) = W_b(x, y, t) + W_s(x, y, t), \tag{17}$$

where $f = z - (\frac{h}{\pi} \sin \frac{\pi z}{h})$. The von Kármán strains by utilizing SSdT can be described as

$$\epsilon_{xx} = \frac{\partial U}{\partial x} - z \frac{\partial^2 W_b}{\partial x^2} - f \frac{\partial^2 W_s}{\partial x^2}, \tag{18}$$

$$\epsilon_{yy} = \frac{\partial V}{\partial y} - z \frac{\partial^2 W_b}{\partial y^2} - f \frac{\partial^2 W_s}{\partial y^2}, \tag{19}$$

$$\epsilon_{xy} = \frac{\partial U}{\partial y} + \frac{\partial V}{\partial x} - 2z \frac{\partial^2 W_b}{\partial x \partial y} - 2f \frac{\partial^2 W_s}{\partial x \partial y}, \tag{20}$$

$$\gamma_{yz} = g \frac{\partial W_s}{\partial y}, \tag{21}$$

$$\gamma_{xz} = g \frac{\partial W_s}{\partial x}, \tag{22}$$

where $g = 1 - \frac{df}{dz} = \cos(\frac{\pi z}{h})$.

4. Motion equations

Fig. 1 depicts a viscoelastic micro plate reinforced with SWCNTs of length a , width b and thickness h . The origin of the reference coordinate system is selected at the corner of the micro plate on the middle plane. The potential energy of structure can be written as

$$U = \frac{1}{2} \int_A \int_{-\frac{h}{2}}^{\frac{h}{2}} (\sigma_{xx} \epsilon_{xx} + \sigma_{yy} \epsilon_{yy} + \sigma_{xy} \gamma_{xy} + \sigma_{xz} \gamma_{xz} + \sigma_{yz} \gamma_{yz}) dz dA \tag{23}$$

Substituting Eqs. (18)-(22) into Eq. (23) leads to

$$\begin{aligned} U = \frac{1}{2} \int_A \left(N_{xx} \frac{\partial u}{\partial x} + N_{xy} \frac{\partial u}{\partial y} + N_{yx} \frac{\partial v}{\partial x} \right. \\ \left. + N_{yy} \frac{\partial v}{\partial y} + Q_x \frac{\partial w_s}{\partial x} + Q_y \frac{\partial w_s}{\partial y} - M_{xxS} \frac{\partial^2 w_s}{\partial x^2} \right. \\ \left. - M_{yyS} \frac{\partial^2 w_s}{\partial y^2} - 2M_{xyS} \frac{\partial^2 w_s}{\partial y \partial x} - M_{xxB} \frac{\partial^2 w_b}{\partial x^2} \right. \\ \left. - M_{yyB} \frac{\partial^2 w_b}{\partial y^2} - 2M_{xyB} \frac{\partial^2 w_b}{\partial y \partial x} \right) dA, \tag{24} \end{aligned}$$

where N , M and Q are the stress resultant–displacement can be defined by

$$\left(N_{xx}, N_{yy}, N_{xy}\right) = \int_{-\frac{h}{2}}^{\frac{h}{2}} \left(\sigma_{xx}^{nl}, \sigma_{yy}^{nl}, \sigma_{xy}^{nl}\right) dz, \quad (25)$$

$$\left(M_{xxB}, M_{yyB}, M_{xyB}\right) = \int_{-\frac{h}{2}}^{\frac{h}{2}} \left(\sigma_{xz}^{nl}, \sigma_{yz}^{nl}, \sigma_{xy}^{nl}\right) z dz, \quad (26)$$

$$\left(M_{xxS}, M_{yyS}, M_{xyS}\right) = -\int_{-\frac{h}{2}}^{\frac{h}{2}} \left(\sigma_{xz}^{nl}, \sigma_{yz}^{nl}, \sigma_{xy}^{nl}\right) f dz, \quad (27)$$

$$\left(Q_x, Q_y\right) = \int_{-\frac{h}{2}}^{\frac{h}{2}} \left(\sigma_{xz}^{nl}, \sigma_{yz}^{nl}\right) g dz, \quad (28)$$

The kinetic energy of nano-composite micro plate can be written as

$$K = \frac{1}{2} \rho \int_A \int_{-\frac{h}{2}}^{\frac{h}{2}} \left(\left(\frac{\partial U_1}{\partial t} \right)^2 + \left(\frac{\partial U_2}{\partial t} \right)^2 + \left(\frac{\partial U_3}{\partial t} \right)^2 \right) dz dA. \quad (29)$$

where ρ is the density of structure.

The external work due to surrounding orthotropic visco-Pasternak medium can be written as

$$W = -\int_A (q) u_3 dA, \quad (30)$$

where

$$q = kw + c_d \dot{w} - G_\xi (\cos^2 \theta w_{,xx} + 2 \cos \theta \sin \theta w_{,xy} + \sin^2 \theta w_{,yy}) - G_\eta (\sin^2 \theta w_{,xx} - 2 \sin \theta \cos \theta w_{,xy} + \cos^2 \theta w_{,yy}), \quad (31)$$

where angle θ describes the local ξ direction of orthotropic foundation with respect to the global x -axis of the plate; k , G_ξ and G_η are Winkler foundation parameter, shear foundation parameters in ξ and η directions, respectively. Finally, applying Hamilton's principle, the motion equations can be obtained as

$$\frac{\partial}{\partial x} N_{xx} + \frac{\partial}{\partial y} N_{xy} - I_0 \frac{\partial^2 U}{\partial t^2} + I_1 \frac{\partial^3 W_b}{\partial x \partial t^2} + J_1 \frac{\partial^3 W_s}{\partial x \partial t^2} = 0, \quad (32)$$

$$\frac{\partial}{\partial x} N_{xy} + \frac{\partial}{\partial y} N_{yy} - I_0 \frac{\partial^2 V}{\partial t^2} + I_1 \frac{\partial^3 W_b}{\partial y \partial t^2} + J_1 \frac{\partial^3 W_s}{\partial y \partial t^2} = 0, \quad (33)$$

$$\begin{aligned} & \frac{\partial^2}{\partial x^2} M_{xxB} + 2 \frac{\partial^2}{\partial x \partial y} M_{xyB} + \frac{\partial^2}{\partial y^2} M_{yyB} + q \\ & + N_x^m \left(\frac{\partial^3 W_b}{\partial x^2} + \frac{\partial^3 W_s}{\partial x^2} \right) + N_y^m \left(\frac{\partial^3 W_b}{\partial y^2} + \frac{\partial^3 W_s}{\partial y^2} \right) \\ & - I_0 \left(\frac{\partial^3 W_b}{\partial t^2} + \frac{\partial^3 W_s}{\partial t^2} \right) - I_1 \left(\frac{\partial^3 U}{\partial x \partial t^2} + \frac{\partial^3 V}{\partial y \partial t^2} \right) \\ & + I_2 \left(\frac{\partial^4 W_b}{\partial x^2 \partial t^2} + \frac{\partial^4 W_b}{\partial y^2 \partial t^2} \right) + J_2 \left(\frac{\partial^4 W_s}{\partial x^2 \partial t^2} + \frac{\partial^4 W_s}{\partial y^2 \partial t^2} \right) = 0, \end{aligned} \quad (34)$$

$$\begin{aligned} & \frac{\partial^2}{\partial x^2} M_{xxS} + 2 \frac{\partial^2}{\partial x \partial y} M_{xyS} + \frac{\partial^2}{\partial y^2} M_{yyS} + \frac{\partial}{\partial x} Q_x + \frac{\partial}{\partial y} Q_y \\ & + q + N_x^m \left(\frac{\partial^3 W_b}{\partial x^2} + \frac{\partial^3 W_s}{\partial x^2} \right) + N_y^m \left(\frac{\partial^3 W_b}{\partial y^2} + \frac{\partial^3 W_s}{\partial y^2} \right) \\ & - I_0 \left(\frac{\partial^3 W_b}{\partial t^2} + \frac{\partial^3 W_s}{\partial t^2} \right) - J_1 \left(\frac{\partial^3 U}{\partial x \partial t^2} + \frac{\partial^3 V}{\partial y \partial t^2} \right) \\ & + J_2 \left(\frac{\partial^4 W_b}{\partial x^2 \partial t^2} + \frac{\partial^4 W_b}{\partial y^2 \partial t^2} \right) + K_2 \left(\frac{\partial^4 W_s}{\partial x^2 \partial t^2} + \frac{\partial^4 W_s}{\partial y^2 \partial t^2} \right) = 0, \end{aligned} \quad (35)$$

where the mass inertias can be defined as

$$\left(I_0, I_1, I_2, J_1, J_2, K_2\right) = \int_{-\frac{h}{2}}^{\frac{h}{2}} \rho \left(1, z, f, zf, z^2, f^2\right) dz. \quad (36)$$

By substituting Eq. (13)-(22) into Eqs. (25)-(28) the stress resultants are obtained as

$$\begin{aligned} N_{xx} &= A_{11} \frac{\partial}{\partial x} U - A_{11z} \frac{\partial^2}{\partial x^2} W_b - A_{11f} \frac{\partial^2}{\partial x^2} W_s \\ & + A_{12} \frac{\partial}{\partial y} V - A_{12z} \frac{\partial^2}{\partial y^2} W_b - A_{12f} \frac{\partial^2}{\partial y^2} W_s + \\ G & \left[\begin{aligned} & A_{11} \frac{\partial^2}{\partial x \partial t} U - A_{11z} \frac{\partial^3}{\partial x^2 \partial t} W_b - A_{11f} \frac{\partial^3}{\partial x^2 \partial t} W_s \\ & + A_{12} \frac{\partial^2}{\partial y \partial t} V - A_{12z} \frac{\partial^3}{\partial y^2 \partial t} W_b - A_{12f} \frac{\partial^3}{\partial y^2 \partial t} W_s \end{aligned} \right], \end{aligned} \quad (37)$$

$$\begin{aligned} N_{yy} &= A_{21} \frac{\partial}{\partial x} U - A_{21z} \frac{\partial^2}{\partial x^2} W_b - A_{21f} \frac{\partial^2}{\partial x^2} W_s \\ & + A_{22} \frac{\partial}{\partial y} V - A_{22z} \frac{\partial^2}{\partial y^2} W_b - A_{22f} \frac{\partial^2}{\partial y^2} W_s + \\ G & \left[\begin{aligned} & A_{12} \frac{\partial^2}{\partial x \partial t} U - A_{12z} \frac{\partial^3}{\partial x^2 \partial t} W_b - A_{12f} \frac{\partial^3}{\partial x^2 \partial t} W_s \\ & + A_{22} \frac{\partial^2}{\partial y \partial t} V - A_{22z} \frac{\partial^3}{\partial y^2 \partial t} W_b - A_{22f} \frac{\partial^3}{\partial y^2 \partial t} W_s \end{aligned} \right], \end{aligned} \quad (38)$$

$$\begin{aligned} N_{xy} &= A_{44} \frac{\partial}{\partial y} U + A_{44} \frac{\partial}{\partial x} V - 2A_{44z} \frac{\partial^2}{\partial x \partial y} W_b - 2A_{44f} \frac{\partial^2}{\partial x \partial y} W_s \\ & + G \left[\begin{aligned} & A_{44} \frac{\partial^2}{\partial y \partial t} U + A_{44} \frac{\partial^2}{\partial x \partial t} V \\ & - 2A_{44z} \frac{\partial^3}{\partial x \partial y \partial t} W_b - 2A_{44f} \frac{\partial^3}{\partial x \partial y \partial t} W_s \end{aligned} \right], \end{aligned} \quad (39)$$

$$Q_x = A_{55g} \frac{\partial}{\partial x} W_s + GA_{55g} \frac{\partial^2}{\partial x \partial t} W_s, \quad (40)$$

$$Q_y = A_{66g} \frac{\partial}{\partial y} W_s + GA_{66g} \frac{\partial^2}{\partial y \partial t} W_s, \quad (41)$$

$$\begin{aligned}
 M_{xxB} &= A_{11z} \frac{\partial}{\partial x} U - B_{11} \frac{\partial^2}{\partial x^2} W_b - A_{11zf} \frac{\partial^2}{\partial x^2} W_s \\
 &+ A_{12z} \frac{\partial}{\partial y} V - B_{12} \frac{\partial^2}{\partial y^2} W_b - A_{12zf} \frac{\partial^2}{\partial y^2} W_s + \\
 G &\left[\begin{aligned} &A_{11z} \frac{\partial^2}{\partial x \partial t} U - B_{11} \frac{\partial^3}{\partial x^2 \partial t} W_b - A_{11zf} \frac{\partial^3}{\partial x^2 \partial t} W_s \\ &+ A_{12z} \frac{\partial^2}{\partial y \partial t} V - B_{12} \frac{\partial^3}{\partial y^2 \partial t} W_b - A_{12zf} \frac{\partial^3}{\partial y^2 \partial t} W_s \end{aligned} \right], \tag{42}
 \end{aligned}$$

$$\begin{aligned}
 M_{xxS} &= A_{11f} \frac{\partial}{\partial x} U - A_{11zf} \frac{\partial^2}{\partial x^2} W_b - E_{11} \frac{\partial^2}{\partial x^2} W_s \\
 &+ A_{12f} \frac{\partial}{\partial y} V - A_{12zf} \frac{\partial^2}{\partial y^2} W_b - E_{12} \frac{\partial^2}{\partial y^2} W_s + \\
 G &\left[\begin{aligned} &A_{11f} \frac{\partial^2}{\partial x \partial t} U - A_{11zf} \frac{\partial^3}{\partial x^2 \partial t} W_b - E_{11} \frac{\partial^3}{\partial x^2 \partial t} W_s \\ &+ A_{12f} \frac{\partial^2}{\partial y \partial t} V - A_{12zf} \frac{\partial^3}{\partial y^2 \partial t} W_b - E_{12} \frac{\partial^3}{\partial y^2 \partial t} W_s \end{aligned} \right], \tag{43}
 \end{aligned}$$

$$\begin{aligned}
 M_{yyB} &= A_{21z} \frac{\partial}{\partial x} U - B_{21} \frac{\partial^2}{\partial x^2} W_b - A_{21zf} \frac{\partial^2}{\partial x^2} W_s \\
 &+ A_{22z} \frac{\partial}{\partial y} V - B_{22} \frac{\partial^2}{\partial y^2} W_b - A_{22zf} \frac{\partial^2}{\partial y^2} W_s + \\
 G &\left[\begin{aligned} &A_{21z} \frac{\partial^2}{\partial x \partial t} U - B_{21} \frac{\partial^3}{\partial x^2 \partial t} W_b - A_{21zf} \frac{\partial^3}{\partial x^2 \partial t} W_s \\ &+ A_{22z} \frac{\partial^2}{\partial y \partial t} V - B_{22} \frac{\partial^3}{\partial y^2 \partial t} W_b - A_{22zf} \frac{\partial^3}{\partial y^2 \partial t} W_s \end{aligned} \right], \tag{44}
 \end{aligned}$$

$$\begin{aligned}
 M_{yyS} &= A_{21f} \frac{\partial}{\partial x} U - A_{21zf} \frac{\partial^2}{\partial x^2} W_b - E_{21} \frac{\partial^2}{\partial x^2} W_s \\
 &+ A_{22f} \frac{\partial}{\partial y} V - A_{22zf} \frac{\partial^2}{\partial y^2} W_b - E_{22} \frac{\partial^2}{\partial y^2} W_s + \\
 G &\left[\begin{aligned} &A_{21f} \frac{\partial^2}{\partial x \partial t} U - A_{21zf} \frac{\partial^3}{\partial x^2 \partial t} W_b - E_{21} \frac{\partial^3}{\partial x^2 \partial t} W_s \\ &+ A_{22f} \frac{\partial^2}{\partial y \partial t} V - A_{22zf} \frac{\partial^3}{\partial y^2 \partial t} W_b - E_{22} \frac{\partial^3}{\partial y^2 \partial t} W_s \end{aligned} \right], \tag{45}
 \end{aligned}$$

$$\begin{aligned}
 M_{xyB} &= 2A_{44z} \frac{\partial}{\partial y} U + 2A_{44z} \frac{\partial}{\partial x} V \\
 &- 2B_{44} \frac{\partial^2}{\partial x \partial y} W_b - 2A_{44zf} \frac{\partial^2}{\partial x \partial y} W_s + \\
 G &\left[\begin{aligned} &2A_{44z} \frac{\partial^2}{\partial y \partial t} U + 2A_{44z} \frac{\partial^2}{\partial x \partial t} V \\ &- 2B_{44} \frac{\partial^3}{\partial x \partial y \partial t} W_b - 2A_{44zf} \frac{\partial^3}{\partial x \partial y \partial t} W_s \end{aligned} \right], \tag{46}
 \end{aligned}$$

$$\begin{aligned}
 M_{xyS} &= 2A_{44f} \frac{\partial}{\partial y} U + 2A_{44f} \frac{\partial}{\partial x} V \\
 &- 2A_{44zf} \frac{\partial^2}{\partial x \partial y} W_b - 2E_{44} \frac{\partial^2}{\partial x \partial y} W_s + \\
 G &\left[\begin{aligned} &2A_{44f} \frac{\partial^2}{\partial y \partial t} U + 2A_{44f} \frac{\partial^2}{\partial x \partial t} V \\ &- 2A_{44zf} \frac{\partial^3}{\partial x \partial y \partial t} W_b - 2E_{44} \frac{\partial^3}{\partial x \partial y \partial t} W_s \end{aligned} \right], \tag{47}
 \end{aligned}$$

$$(A_{11}, A_{12}, A_{22}, A_{44}) = \sum_{k=1}^N \int_{z^{(k-1)}}^{z^{(k)}} (C_{11}^{(k)}, C_{12}^{(k)}, C_{22}^{(k)}, C_{44}^{(k)}) dz, \tag{48}$$

$$(A_{11z}, A_{12z}, A_{22z}, A_{44z}) = \sum_{k=1}^N \int_{z^{(k-1)}}^{z^{(k)}} (C_{11}^{(k)}, C_{12}^{(k)}, C_{22}^{(k)}, C_{44}^{(k)}) z dz, \tag{49}$$

$$(A_{11f}, A_{12f}, A_{22f}, A_{44f}) = \sum_{k=1}^N \int_{z^{(k-1)}}^{z^{(k)}} (C_{11}^{(k)}, C_{12}^{(k)}, C_{22}^{(k)}, C_{44}^{(k)}) f dz, \tag{50}$$

$$(A_{11zf}, A_{12zf}, A_{22zf}, A_{44zf}) = \sum_{k=1}^N \int_{z^{(k-1)}}^{z^{(k)}} (C_{11}^{(k)}, C_{12}^{(k)}, C_{22}^{(k)}, C_{44}^{(k)}) z f dz, \tag{51}$$

$$(A_{55g}, A_{66g}) = \sum_{k=1}^N \int_{z^{(k-1)}}^{z^{(k)}} (C_{55}^{(k)}, C_{66}^{(k)}) dz, \tag{52}$$

$$(B_{11}, B_{12}, B_{22}, B_{44}) = \sum_{k=1}^N \int_{z^{(k-1)}}^{z^{(k)}} (C_{11}^{(k)}, C_{12}^{(k)}, C_{22}^{(k)}, C_{44}^{(k)}) z^2 dz, \tag{53}$$

$$(E_{11}, E_{12}, E_{22}, E_{44}) = \sum_{k=1}^N \int_{z^{(k-1)}}^{z^{(k)}} (C_{11}^{(k)}, C_{12}^{(k)}, C_{22}^{(k)}, C_{44}^{(k)}) f^2 dz, \tag{54}$$

By substituting Eqs. (32)-(35) into Eqs. (37)-(47), the equations of motion can be expressed as

$$\begin{aligned}
 &\left(\begin{aligned} &A_{11} \frac{\partial}{\partial x} U - A_{11z} \frac{\partial^2}{\partial x^2} W_b - A_{11f} \frac{\partial^2}{\partial x^2} W_s + A_{12} \frac{\partial}{\partial y} V \\ &- A_{12z} \frac{\partial^2}{\partial y^2} W_b - A_{12f} \frac{\partial^2}{\partial y^2} W_s + \\ &G \left[\begin{aligned} &A_{11} \frac{\partial^2}{\partial x \partial t} U - A_{11z} \frac{\partial^3}{\partial x^2 \partial t} W_b - A_{11f} \frac{\partial^3}{\partial x^2 \partial t} W_s \\ &+ A_{12} \frac{\partial^2}{\partial y \partial t} V - A_{12z} \frac{\partial^3}{\partial y^2 \partial t} W_b - A_{12f} \frac{\partial^3}{\partial y^2 \partial t} W_s \end{aligned} \right] \end{aligned} \right) \\
 &+ \frac{\partial}{\partial y} \left(\begin{aligned} &A_{44} \frac{\partial}{\partial y} U + A_{44} \frac{\partial}{\partial x} V - 2A_{44z} \frac{\partial^2}{\partial x \partial y} W_b \\ &- 2A_{44f} \frac{\partial^2}{\partial x \partial y} W_s + G \left[\begin{aligned} &A_{44} \frac{\partial^2}{\partial y \partial t} U + A_{44} \frac{\partial^2}{\partial x \partial t} V \\ &- 2A_{44z} \frac{\partial^3}{\partial x \partial y \partial t} W_b - 2A_{44f} \frac{\partial^3}{\partial x \partial y \partial t} W_s \end{aligned} \right] \end{aligned} \right) \\
 &= (1 - \mu V^2) \left[I_0 \frac{\partial^2 U}{\partial t^2} - I_1 \frac{\partial^3 W_b}{\partial x \partial t^2} - J_1 \frac{\partial^3 W_s}{\partial x \partial t^2} \right], \tag{55}
 \end{aligned}$$

$$\frac{\partial}{\partial x} \left[\begin{array}{l} A_{44} \frac{\partial}{\partial y} U + A_{44} \frac{\partial}{\partial x} V - 2A_{44z} \frac{\partial^2}{\partial x \partial y} W_b \\ -2A_{44f} \frac{\partial^2}{\partial x \partial y} W + G \left[\begin{array}{l} A_{44} \frac{\partial^2}{\partial y \partial t} U + A_{44} \frac{\partial^2}{\partial x \partial t} V \\ -2A_{44z} \frac{\partial^3}{\partial x \partial y \partial t} W_b - 2A_{44f} \frac{\partial^3}{\partial x \partial y \partial t} W_s \end{array} \right] \end{array} \right] \\ + \frac{\partial}{\partial y} \left[\begin{array}{l} A_{21} \frac{\partial}{\partial x} U - A_{21z} \frac{\partial^2}{\partial x^2} W_b - A_{21f} \frac{\partial^2}{\partial x^2} W_s \\ + A_{22} \frac{\partial}{\partial y} V - A_{22z} \frac{\partial^2}{\partial y^2} W_b - A_{22f} \frac{\partial^2}{\partial y^2} W_s + \\ G \left[\begin{array}{l} A_{12} \frac{\partial^2}{\partial x \partial t} U - A_{12z} \frac{\partial^3}{\partial x^2 \partial t} W_b - A_{12f} \frac{\partial^3}{\partial x^2 \partial t} W_s \\ + A_{22} \frac{\partial^2}{\partial y \partial t} V - A_{22z} \frac{\partial^3}{\partial y^2 \partial t} W_b - A_{22f} \frac{\partial^3}{\partial y^2 \partial t} W_s \end{array} \right] \end{array} \right] \\ = (1 - \mu \nabla^2) \left[I_0 \frac{\partial^3 V}{\partial t^2} - I_1 \frac{\partial^3 W_b}{\partial y \partial t^2} - J_1 \frac{\partial^3 W_s}{\partial y \partial t^2} \right], \tag{56}$$

$$\frac{\partial^2}{\partial x^2} \left[\begin{array}{l} A_{11z} \frac{\partial}{\partial x} U - B_{11} \frac{\partial^2}{\partial x^2} W_b - A_{11f} \frac{\partial^2}{\partial x^2} W_s + A_{12z} \frac{\partial}{\partial y} V \\ - B_{12} \frac{\partial^2}{\partial y^2} W_b - A_{12f} \frac{\partial^2}{\partial y^2} W_s + \\ G \left[\begin{array}{l} A_{11z} \frac{\partial^2}{\partial x \partial t} U - B_{11} \frac{\partial^3}{\partial x^2 \partial t} W_b - A_{11f} \frac{\partial^3}{\partial x^2 \partial t} W_s \\ + A_{12z} \frac{\partial^2}{\partial y \partial t} V - B_{12} \frac{\partial^3}{\partial y^2 \partial t} W_b - A_{12f} \frac{\partial^3}{\partial y^2 \partial t} W_s \end{array} \right] \end{array} \right] \\ + 2 \frac{\partial^2}{\partial x \partial y} \left[\begin{array}{l} 2A_{44z} \frac{\partial}{\partial y} U + 2A_{44z} \frac{\partial}{\partial x} V - 2B_{44} \frac{\partial^2}{\partial x \partial y} W_b \\ - 2A_{44f} \frac{\partial^2}{\partial x \partial y} W_s + G \left[\begin{array}{l} 2A_{44z} \frac{\partial^2}{\partial y \partial t} U + 2A_{44z} \frac{\partial^2}{\partial x \partial t} V \\ - 2B_{44} \frac{\partial^3}{\partial x \partial y \partial t} W_b - 2A_{44f} \frac{\partial^3}{\partial x \partial y \partial t} W_s \end{array} \right] \end{array} \right] \\ + \frac{\partial^2}{\partial y^2} \left[\begin{array}{l} A_{21z} \frac{\partial}{\partial x} U - B_{21} \frac{\partial^2}{\partial x^2} W_b - A_{21f} \frac{\partial^2}{\partial x^2} W_s \\ + A_{22z} \frac{\partial}{\partial y} V - B_{22} \frac{\partial^2}{\partial y^2} W_b - A_{22f} \frac{\partial^2}{\partial y^2} W_s + \\ G \left[\begin{array}{l} A_{21z} \frac{\partial^2}{\partial x \partial t} U - B_{21} \frac{\partial^3}{\partial x^2 \partial t} W_b - A_{21f} \frac{\partial^3}{\partial x^2 \partial t} W_s \\ + A_{22z} \frac{\partial^2}{\partial y \partial t} V - B_{22} \frac{\partial^3}{\partial y^2 \partial t} W_b - A_{22f} \frac{\partial^3}{\partial y^2 \partial t} W_s \end{array} \right] \end{array} \right] \\ (1 - \mu \nabla^2) \left[-kw - c_y w + G_z (\cos^2 \theta w_{,xx} + 2 \cos \theta \sin \theta w_{,xy} + \sin^2 \theta w_{,yy}) \right. \\ + G_y (\sin^2 \theta w_{,xx} - 2 \sin \theta \cos \theta w_{,xy} + \cos^2 \theta w_{,yy}) \\ + N_x^m \left(\frac{\partial^3 W_b}{\partial x^2} + \frac{\partial^3 W_s}{\partial x^2} \right) + N_y^m \left(\frac{\partial^3 W_b}{\partial y^2} + \frac{\partial^3 W_s}{\partial y^2} \right) \\ = I_0 \left(\frac{\partial^3 W_b}{\partial t^2} + \frac{\partial^3 W_s}{\partial t^2} \right) + I_1 \left(\frac{\partial^3 U}{\partial x \partial t^2} + \frac{\partial^3 V}{\partial y \partial t^2} \right) \\ \left. - J_2 \left(\frac{\partial^3 W_b}{\partial x^2 \partial t^2} + \frac{\partial^3 W_b}{\partial y^2 \partial t^2} \right) - J_2 \left(\frac{\partial^3 W_s}{\partial x^2 \partial t^2} + \frac{\partial^3 W_s}{\partial y^2 \partial t^2} \right) \right], \tag{57}$$

$$\frac{\partial^2}{\partial x^2} \left[\begin{array}{l} A_{11f} \frac{\partial}{\partial x} U - A_{11f} \frac{\partial^2}{\partial x^2} W_b - E_{11} \frac{\partial^2}{\partial x^2} W_s + A_{12f} \frac{\partial}{\partial y} V \\ - A_{12f} \frac{\partial^2}{\partial y^2} W_b - E_{12} \frac{\partial^2}{\partial y^2} W_s + \\ G \left[\begin{array}{l} A_{11f} \frac{\partial^2}{\partial x \partial t} U - A_{11f} \frac{\partial^3}{\partial x^2 \partial t} W_b - E_{11} \frac{\partial^3}{\partial x^2 \partial t} W_s \\ + A_{12f} \frac{\partial^2}{\partial y \partial t} V - A_{12f} \frac{\partial^3}{\partial y^2 \partial t} W_b - E_{12} \frac{\partial^3}{\partial y^2 \partial t} W_s \end{array} \right] \end{array} \right] \\ + 2 \frac{\partial^2}{\partial x \partial y} \left[\begin{array}{l} 2A_{44f} \frac{\partial}{\partial y} U + 2A_{44f} \frac{\partial}{\partial x} V - 2A_{44z} \frac{\partial^2}{\partial x \partial y} W_b \\ - 2E_{44} \frac{\partial^2}{\partial x \partial y} W + G \left[\begin{array}{l} 2A_{44f} \frac{\partial^2}{\partial y \partial t} U + 2A_{44f} \frac{\partial^2}{\partial x \partial t} V \\ - 2A_{44z} \frac{\partial^3}{\partial x \partial y \partial t} W_b - 2E_{44} \frac{\partial^3}{\partial x \partial y \partial t} W_s \end{array} \right] \end{array} \right] \\ + \frac{\partial^2}{\partial y^2} \left[\begin{array}{l} A_{21f} \frac{\partial}{\partial x} U - A_{21f} \frac{\partial^2}{\partial x^2} W_b - E_{21} \frac{\partial^2}{\partial x^2} W_s + A_{22f} \frac{\partial}{\partial y} V \\ - A_{22f} \frac{\partial^2}{\partial y^2} W_b - E_{22} \frac{\partial^2}{\partial y^2} W_s + \\ G \left[\begin{array}{l} A_{21f} \frac{\partial^2}{\partial x \partial t} U - A_{21f} \frac{\partial^3}{\partial x^2 \partial t} W_b - E_{21} \frac{\partial^3}{\partial x^2 \partial t} W_s \\ + A_{22f} \frac{\partial^2}{\partial y \partial t} V - A_{22f} \frac{\partial^3}{\partial y^2 \partial t} W_b - E_{22} \frac{\partial^3}{\partial y^2 \partial t} W_s \end{array} \right] \end{array} \right] \\ + \frac{\partial}{\partial x} \left(A_{55z} \frac{\partial}{\partial x} W_s + GA_{55z} \frac{\partial^2}{\partial x \partial t} W_s \right) + \frac{\partial}{\partial y} \left(A_{66z} \frac{\partial}{\partial y} W_s + GA_{66z} \frac{\partial^2}{\partial y \partial t} W_s \right) \\ (1 - \mu \nabla^2) \left[-kw - c_y w + G_z (\cos^2 \theta w_{,xx} + 2 \cos \theta \sin \theta w_{,xy} + \sin^2 \theta w_{,yy}) \right. \\ + G_y (\sin^2 \theta w_{,xx} - 2 \sin \theta \cos \theta w_{,xy} + \cos^2 \theta w_{,yy}) \\ + N_x^m \left(\frac{\partial^3 W_b}{\partial x^2} + \frac{\partial^3 W_s}{\partial x^2} \right) + N_y^m \left(\frac{\partial^3 W_b}{\partial y^2} + \frac{\partial^3 W_s}{\partial y^2} \right) \\ = I_0 \left(\frac{\partial^3 W_b}{\partial t^2} + \frac{\partial^3 W_s}{\partial t^2} \right) + J_1 \left(\frac{\partial^3 U}{\partial x \partial t^2} + \frac{\partial^3 V}{\partial y \partial t^2} \right) \\ \left. - J_2 \left(\frac{\partial^3 W_b}{\partial x^2 \partial t^2} + \frac{\partial^3 W_b}{\partial y^2 \partial t^2} \right) - K_2 \left(\frac{\partial^3 W_s}{\partial x^2 \partial t^2} + \frac{\partial^3 W_s}{\partial y^2 \partial t^2} \right) \right], \tag{58}$$

5. GDQM

In this method, the differential equations are changed into a first order algebraic equation by employing appropriate weighting coefficients. Because weighting coefficients do not relate to any special problem and only depend on the grid spacing. In other words, the partial derivatives of a function (say W here) are approximated with respect to specific variables (say x and y), at a discontinuous point in a defined domain ($0 < x < L_x$ and $0 < y < L_y$) as a set of linear weighting coefficients and the amount represented by the function itself at that point and other points throughout the domain. The approximation of the n^{th} and m^{th} derivatives function with respect to x and y , respectively may be expressed in general form as (Lei *et al.* 2013)

$$f_x^{(n)}(x_i, y_i) = \sum_{k=1}^{N_x} A^{(n)}_{ik} f(x_k, y_j), \\ f_y^{(m)}(x_i, y_i) = \sum_{l=1}^{N_y} B^{(m)}_{jl} f(x_i, y_l), \tag{59} \\ f_{xy}^{(n+m)}(x_i, y_i) = \sum_{k=1}^{N_x} \sum_{l=1}^{N_y} A^{(n)}_{ik} B^{(m)}_{jl} f(x_k, y_l),$$

where N_x and N_y , denotes the number of points in x and y directions, $f(x, y)$ is the function and A_{ik}, B_{jl} are the weighting coefficients defined as

$$A^{(1)}_{ij} = \frac{M(x_i)}{(x_i - x_j)M(x_j)},$$

$$B^{(1)}_{ij} = \frac{P(y_i)}{(y_i - y_j)M(y_j)},$$
(60)

where M and P are Lagrangian operators defined as

$$M(x_i) = \prod_{j=1}^{N_x} (x_i - x_j), \quad i \neq j$$

$$P(y_i) = \prod_{j=1}^{N_y} (y_i - y_j), \quad i \neq j.$$
(61)

The weighting coefficients for the second, third and fourth derivatives are determined via matrix multiplication

$$A^{(2)}_{ij} = \sum_{k=1}^{N_x} A^{(1)}_{ik} A^{(1)}_{kj}, \quad A^{(3)}_{ij} = \sum_{k=1}^{N_x} A^{(2)}_{ik} A^{(1)}_{kj},$$

$$A^{(4)}_{ij} = \sum_{k=1}^{N_x} A^{(3)}_{ik} A^{(1)}_{kj}, \quad i, j = 1, 2, \dots, N_x,$$

$$B^{(2)}_{ij} = \sum_{k=1}^{N_y} B^{(1)}_{ik} B^{(1)}_{kj}, \quad B^{(3)}_{ij} = \sum_{k=1}^{N_y} B^{(2)}_{ik} B^{(1)}_{kj},$$

$$B^{(4)}_{ij} = \sum_{k=1}^{N_y} B^{(3)}_{ik} B^{(1)}_{kj}, \quad i, j = 1, 2, \dots, N_y.$$
(62)

Using the following rule, the distribution of grid points in domain is calculated as

$$x_i = \frac{L_x}{2} \left[1 - \cos\left(\frac{\pi i}{N_x}\right) \right],$$

$$y_j = \frac{L_y}{2} \left[1 - \cos\left(\frac{\pi j}{N_y}\right) \right],$$
(63)

Let the in-plane load P be periodic and may be expressed as

$$P(t) = \alpha P_{cr} + \beta P_{cr} \cos(\omega t),$$
(64)

where ω is the frequency of excitation, P_{cr} is the static buckling load, α and β may be defined as static and dynamic load factors, respectively. However, the motion equations can be written as

$$\{[K - \alpha P_{cr} K_G - \beta P_{cr} \cos(\omega t) K_G][d] + [C][\dot{d}] + [M][\ddot{d}]\} = [0],$$
(65)

5.1 Bolotin's method

In order to determinate the boundaries of dynamic instability regions, the method suggested by Bolotin is

applied. Hence, the components of $\{d\}$ can be written in the Fourier series with period $2T$ as

$$\{d\} = \sum_{k=1,3,\dots}^{\infty} \left[\{a\}_k \sin \frac{k\omega t}{2} + \{b\}_k \cos \frac{k\omega t}{2} \right],$$
(66)

According to this method, the first instability region is usually the most important in studies of structures. It is due to the fact that the first DIR is wider than other DIRs and structural damping in higher regions becomes neutralize. Substituting Eq. (66) into Eq. (65) and setting the coefficients of each sine and cosine as well as the sum of the constant terms to zero, yields

$$\left| \begin{pmatrix} [K_L + K_{NL}] - P_{cr} \alpha [K]_G \\ \pm P_{cr} \frac{\beta}{2} [K]_G \mp [C] \frac{\omega}{2} - [M] \frac{\omega^2}{4} \end{pmatrix} \right| = 0,$$
(67)

Solving the above equation based on eigenvalue problem, the variation of ω with respect to α can be plotted as DIR.

6. Results and discussion

A computer program is prepared for the numerical solution of nonlinear buckling of CNTRC sandwich micro plates resting on an orthotropic elastomeric temperature-dependent foundation. Here, Poly methyl methacrylate (PMMA) is selected for the matrix which have constant Poisson's ratios of $\nu_m = 0.34$, temperature-dependent thermal coefficient of $\alpha_m = (1 + 0.0005\Delta T) \times 10^{-6} / K$, and temperature-dependent Young moduli of $E_m = (3.52 - 0.0034T) GPa$ in which $T = T_0 + \Delta T$ and $T_0 = 300 K$ (room temperature). In addition, (10, 10) SWCNTs are selected as reinforcements with the material properties listed in Table 1 (Shen 2009).

The elastomeric medium is made of Poly dimethylsiloxane (PDMS) which the temperature-dependent material properties of which are assumed to be $\nu_s = 0.48$ and $E_s = (3.22 - 0.0034T) GPa$ in which $T = T_0 + \Delta T$ and $T_0 = 300 K$ (room temperature).

Table 1 Temperature-dependent material properties of (10, 10) SWCNT (L= 9.26 nm, R= 0.68 nm, h= 0.067 nm, $\nu_{12}^{CNT} = 0.175$)

T (K)	E_{11}^{CNT} (TPa)	E_{22}^{CNT} (TPa)	G_{12}^{CNT} (TPa)	α_{12}^{CNT} ($10^{-6} / K$)	α_{22}^{CNT} ($10^{-6} / K$)
300	5.6466	7.0800	1.9445	3.4584	5.1682
500	5.5308	6.9348	1.9643	4.5361	5.0189
700	5.4744	6.8641	1.9644	4.6677	4.8943

To the best of the authors' knowledge no published literature is available for viscoelastic nanocomposite sandwich micro plate based on SSDT. Since, no reference to such a work is found to-date in the literature; its validation is not possible. However, in an attempt to validate this work as far as possible, a simplified analysis of this paper is carried out without considering the nonlocal parameter, orthotropic visco-Pasternak foundation, viscoelastic property and SWCNTs as reinforcer. Present results are compared with the work of Lanhe *et al.* (2007) based on First-order shear deformation theory (FSDT). Considering the material properties the same as Lanhe *et al.* (2007) and dimensionless frequency as $\bar{\omega} = \alpha(a/h)^2 \sqrt{\rho_m(1-\nu^2)/E_m}$, the results of comparison are shown in Fig. 2. As can be seen, present results are in good agreement with Lanhe *et al.* (2007), indication validation of this work. Noted that the little difference between this work and Lanhe *et al.* (2007) is due to considering thermal load in Lanhe *et al.* (2007).

The convergence and accuracy of the DQM in calculating the excitation frequency of the CNTRC sandwich micro plates is shown in Fig. 3. Fast rate of convergence of the method are quite evident and it is found that 15 DQ grid points can yield accurate results.

In realizing the influence of CNTs as reinforce, Fig. 4 is plotted. This figure shows the effects of CNTs volume fraction on the dimensionless excitation frequency ($\Omega = \alpha(a/h)^2 \sqrt{\rho_m(1-\nu^2)/E_m}$) with respect to dynamic load amplitude. In these figure, the regions inside and outside the boundary curves correspond to unstable (parametric resonance) and stable regions, respectively. As can be seen, with increasing the CNTs volume fraction, the DIR shifts to higher frequencies. In other words, increasing the CNTs volume fraction leads to higher resonance frequency which is due to increase in the stiffness of structure.

Depicted in Fig. 5 is the dimensionless excitation frequency versus dynamic load factor for the UD and three types of FG CNTRC sandwich micro plates.

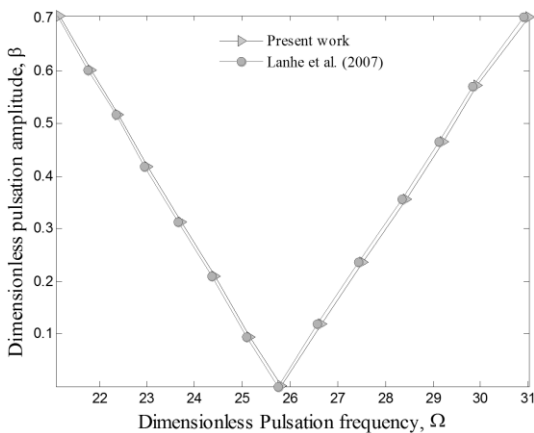


Fig. 2 Comparison of present work with Lanhe *et al.* (2007)

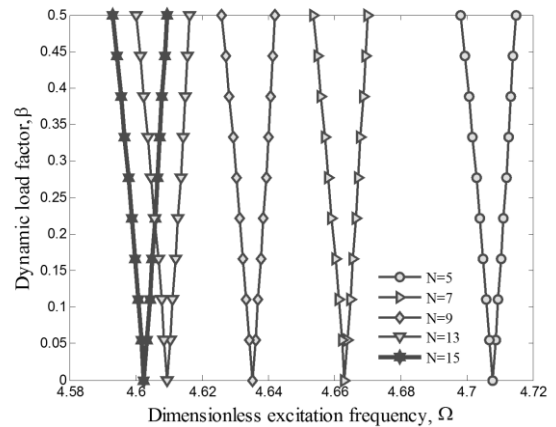


Fig. 3 Convergence of proposed method (DQM)

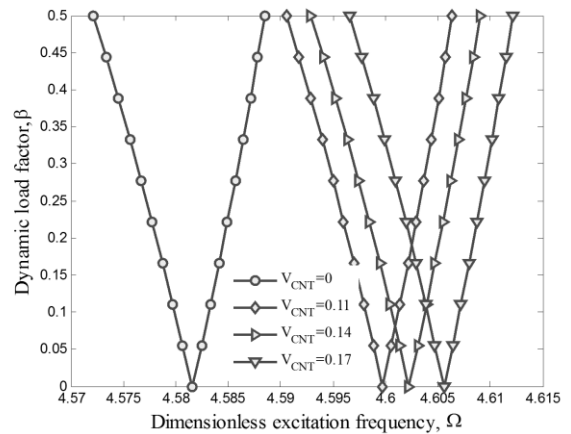


Fig. 4 CNT Volume percent effects on the DIR of FG-CNT-reinforced micro plate

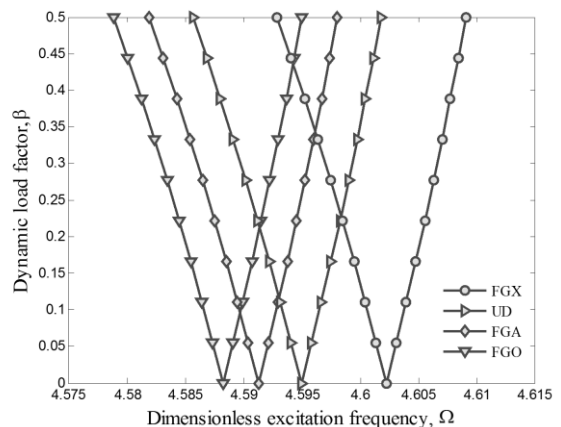


Fig. 5 CNT distribution type effects on the DIR of FG-CNT-reinforced micro plate

It should be noted that the mass fraction (w_{CNT}) of the UD and FG distribution of CNTs in polymer are considered

equal for the purpose of comparisons. As can be seen, the dimensionless excitation frequency of FGA- and FGO-CNTRC sandwich micro plates are lower than those of UD-CNTRC sandwich micro plates while the FGX- CNTRC sandwich micro plate have higher dimensionless excitation frequency with respect to three other cases. It is due to the fact that the stiffness of CNTRC sandwich micro plates changes with the form of CNT distribution in matrix. However, it can be concluded that CNT distribution close to top and bottom are more efficient than those distributed nearby the mid-plane for increasing the stiffness of plates.

The effect of different boundary conditions is presented in Fig. 6 on the dimensionless excitation frequency versus dynamic load factor. It can be found that the CCCC boundary condition yields to higher resonance frequency. In other words, comparing the assumed boundary conditions, the DIR of structure moves to right for the case of micro plate with CCCC boundary conditions.

Fig. 7 demonstrates the effects of nonlocal parameters on the dimensionless excitation frequency versus dynamic load factor. As can be seen, the frequency of the system decreases with considering nonlocal theory. It means that with considering nonlocal parameter, DIR of system happens in lower frequencies. This is because increasing the nonlocal parameter implies decreasing interaction force between micro plate atoms leads to a softer structure.

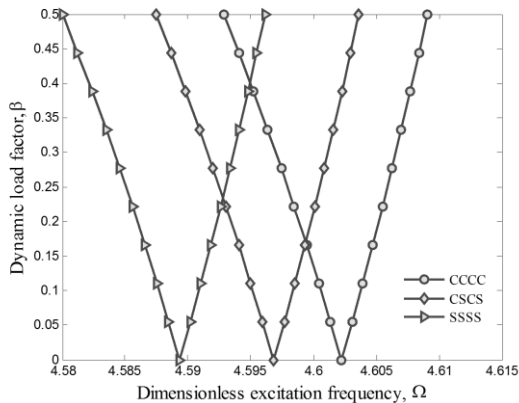


Fig. 6 Boundary condition effects on the DIR of FG-CNT-reinforced micro plate

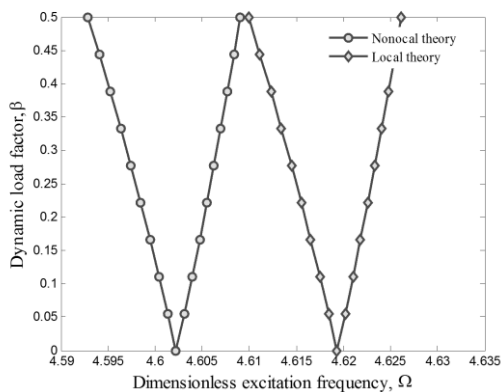


Fig. 7 Nonlocal parameter effects on the DIR of FG-CNT-reinforced micro plate

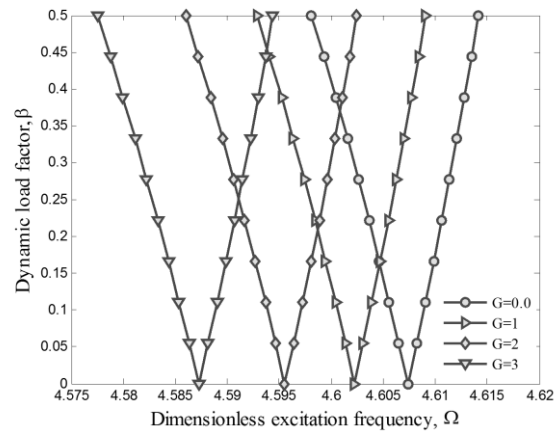


Fig. 8 Structural damping effects on the DIR of FG-CNT-reinforced micro plate

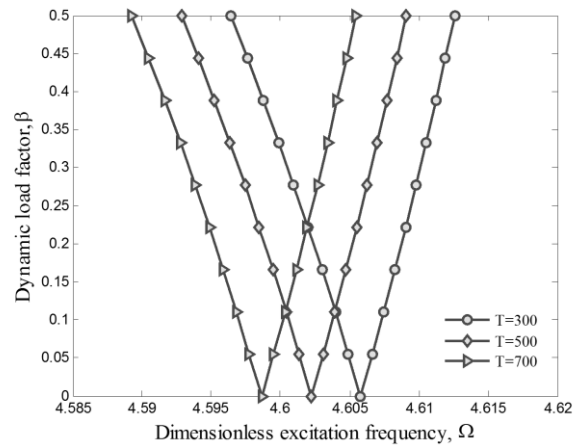


Fig. 9 Temperature effects on the DIR of FG-CNT-reinforced micro plate

Fig. 8 demonstrates the DIR for different structural damping constant. As can be seen, the DIR and frequency of viscoelastic sandwich micro plate are lower than those of non-visco structure (i.e., $G=0$). This remarkable difference show that considering the nature of nanocomposite micro plate as viscoelastic can yield the accurate results with respect to non-visco micro plate. The reason is that assuming viscoelastic micro plate means induce of damping force which results in more absorption of vibration energy by the micro plate.

The effect of temperature on the dimensionless excitation frequency of the CNTRC sandwich micro plate with respect to the dynamic load factor is demonstrated in Fig. 9. It can be found that the dimensionless excitation frequency of structure decreases with increasing temperature which is due to the higher stiffness CNTRC micro plate with lower temperature.

The effect of different viscoelastic mediums is demonstrated in Fig. 10 for four cases which are without viscoelastic medium, visco-Winkler medium, visco-Pasternak medium and orthotropic visco-Pasternak medium.

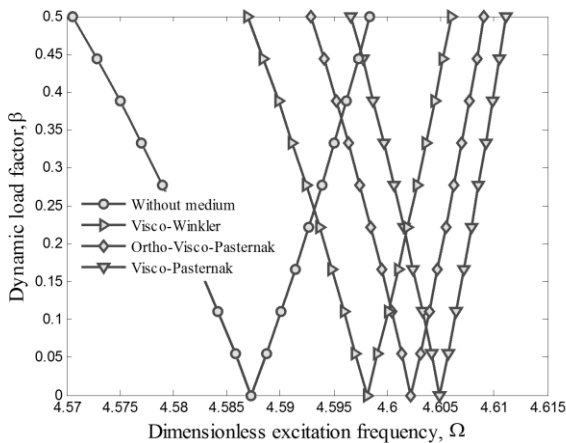


Fig. 10 Viscoelastic medium type effects on the DIR of FG-CNT-reinforced micro plate

It can be seen that considering viscoelastic medium increases the excitation frequency of structure and DIR shifts to higher frequencies. It is due to the fact that considering viscoelastic medium leads to stiffer structure. Furthermore, the excitation frequency which leads to DIR for the case of visco-Pasternak medium is higher than the visco-Winkler medium. It is because in the visco-Pasternak medium indeed the normal loads, the shear forces are considered. In addition, the DIR of orthotropic visco-Pasternak medium is behind the DIR of visco-Pasternak one since the shear layer is considered with the angle of 30 degree.

7. Conclusions

Considering different distribution type for CNTs, the dynamic buckling of viscoelastic temperature-dependent nanocomposite sandwich micro plates was presented. The sandwich micro plate is reinforced with SWCNTs which the equivalent material properties were obtained by mixture model. Orthotropic viscoelastic foundation was used for simulating the surrounding elastic medium. The SSDT was applied for mathematical modeling of structure considering size effects using Eringen's nonlocal theory. DQ method in conjunction with the Bolotin's method was applied for obtaining the DIR of structure so that the effects of different parameters such as volume percent of SWCNTs, distribution type of CNTs, temperature, volume percent of SWCNTs in volume, nonlocal parameter and structural damping were shown. Results depict that considering the nature of structure as viscoelastic can yield the accurate results with respect to non-visco one. Furthermore, the frequency of the system decreases considering the nonlocal parameter. In addition, with increasing the CNTs volume fraction, the DIR shifts to higher frequencies. Furthermore, FGX distribution of CNTs leads to higher frequency. The results of this study were in good agreement with those reported by Lanhe *et al.* (2007). The results presented in this work can be useful for the study and design of the next

generation of nanocomposite structures that make use of the nonlocal dynamic instability of viscoelastic microplate.

References

- Abdollahzadeh Shahrabaki, E. and Alibeigloo, A. (2014), "Three-dimensional free vibration of carbon nanotube-reinforced composite plates with various boundary conditions using Ritz method", *Compos. Struct.*, **111**, 362-370.
- Atteshamuddin, S.S. and Yuwaraj, M.Gh. (2017), "On the free vibration of angle-ply laminated composite and soft core sandwich plates", *Int. J. Sandw. Struct.*, In press.
- Chetan, S.J., Madhusudan, M., Vidyashankar, S. and Charles Lu, Y. (2017), "Modelling of the interfacial damping due to nanotube agglomerations in nanocomposites", *Smart Struct. Syst.*, **19**(1), 57-66.
- Eringen, A.C. (1983), "On differential equations of nonlocal elasticity and solutions of screw dislocation and surface waves", *J. Appl. Phys.*, **54**(9), 703-710.
- Ke, L.L., Liu, C. and Wang, Y.S. (2015), "Free vibration of nonlocal piezoelectric nanoplates under various boundary conditions", *Physica E*, **66**, 93-106.
- Kiani, K. (2014), "Free vibration of conducting nanoplates exposed to unidirectional in-plane magnetic fields using nonlocal shear deformable plate theories", *Physica E*, **57**, 179-192.
- Lanhe, W., Wang, H. and Wang, D. (2007), "Dynamic stability analysis of FGM plates by the moving leastsquares differential quadrature method", *Compos. Struct.*, **77**(3), 383-394.
- Lei, Y., Adhikari, S. and Friswell, M.I. (2013), "Vibration of nonlocal Kelvin-Voigt viscoelastic damped Timoshenko beams", *Int. J. Eng. Sci.*, **66-67**, 1-13.
- Li, Y.S., Cai, Z.Y. and Shi, S.Y. (2014), "Buckling and free vibration of magneto-electroelastic nanoplate based on nonlocal theory", *Compos. Struct.*, **111**, 522-529.
- Mantari, J.L. and Guedes Soares, C. (2014), "Four-unknown quasi-3D shear deformation theory for advanced composite plates", *Compos. Struct.*, **109**, 231-9.
- Mori, T. and Tanaka, K. (1973), "Average stress in matrix and average elastic energy of materials with misfitting inclusions", *Acta Metal. Mater.*, **21**(5), 571-574.
- Natarajan, S., Haboussi, M. and Manickam, G. (2014), "Application of higher-order structural theory to bending and free vibration analysis of sandwich plates with CNT reinforced composite facesheets", *Compos. Struct.*, **113**, 197-207.
- Pandit, M.K., Sheikh, A.H. and Singh, B.N. (2009), "Analysis of laminated sandwich plates based on an improved higher order zigzag theory", *Int. J. Sandw. Struct.*, **12**(3), 307-326.
- Phung-Van, P., Abdel-Wahab, M. and Liew, K.M. (2017), "Isogeometric analysis of functionally graded carbon nanotube-reinforced composite plates using higher-order shear deformation theory", *Compos. Struct.*, **123**, 137-149.
- Rafiee, M., He, X.Q. and Liew, K.M. (2014), "Non-linear dynamic stability of piezoelectric functionally graded carbon nanotube-reinforced composite plates with initial geometric imperfection", *Int. J. Nonlinear Mech.*, **59**, 37-51.
- Shen, H.S. (2009), "Nonlinear bending of functionally graded carbon nanotube-reinforced composite plates in thermal environments", *Compo. Struct.*, **91**(1), 9-19.
- Thai, H.T. and Vo, T.P. (2013), "A new sinusoidal shear deformation theory for bending buckling and vibration of functionally graded plates", *Appl. Math. Model.*, **37**(5), 3269-3281.
- Wattanasakulpong, N. and Chaikittiratanana, A. (2015), "Exact solutions for static and dynamic analyses of carbon nanotube-

reinforced composite plates with Pasternak elastic foundation”, *Appl. Math. Model.*, **39**(18), 5459-5472.

Ying, Z.G., Ni, Y.Q. and Duan, Y.F. (2017), “Stochastic micro-vibration response characteristics of a sandwich plate with MR visco-elastomer core and mass”, *Smart Struct. Syst.*, **16**(1), 141-162.

CC